*remote sensing*

MDPI

*Article*

# Spatial–Temporal Trends in and Attribution Analysis of Vegetation Change in the Yellow River Basin, China

**Shengqi Jian, Qiankun Zhang and Huiliang Wang ***

Yellow River Laboratory, Zhengzhou University, Zhengzhou 450001, China
* Correspondence: wanghuiliang@zzu.edu.cn; Tel.: +86-18623048694

**Abstract:** In 1999, the Yellow River Basin (YRB) launched the Grain for Green Program (GGP), which has had a huge impact on the Yellow River Basin vegetation. Research regarding the causes of vegetation changes can provide beneficial information for the management and construction of the ecological environment in the Yellow River Basin. In this study, after reconstructing the relationship between vegetation and climate change under natural conditions, topographic factors were introduced to understand vegetation change in the Yellow River Basin before and after the initiation of the Grain for Green Program, and the contribution rates of the driving factors of change were analyzed. Results show that human activities have had a great impact on the vegetation cover in the Yellow River Basin. We found that after the start of the Grain for Green Program, the vegetation recovery rate was more than six times (slope = 0.0067) that before its start (slope = 0.0011); high NDVI levels moved to lower altitudes, while low NDVI levels moved to high altitudes; and most vegetation types turned to gentle slopes. Human activities and climate change are the dominant factors influencing vegetation coverage, and the contribution rate of human activities had reached 59.3% after 2000, with a tendency to gradually dominate.

**Keywords:** Yellow River Basin; climate change; human activities; attribution; contribution



**Citation:** Jian, S.; Zhang, Q.; Wang, H. Spatial–Temporal Trends in and Attribution Analysis of Vegetation Change in the Yellow River Basin, China. *Remote Sens.* **2022**, *14*, 4607. https://doi.org/10.3390/rs14184607

Academic Editor: Qinghua Guo

Received: 6 August 2022
Accepted: 9 September 2022
Published: 15 September 2022



## 1. Introduction

Vegetation is an important part of the terrestrial ecosystem, playing an important role in responding to climate change conditions, improving the ecological environment, and promoting water circulation [1]. Therefore, to understand ecological changes and improve the ecological environment, research on spatial–temporal variation trends in and driving factors behind vegetation is of great importance [2]. Research shows that since the 1980s, the droughts caused by the temperature rise in the northern hemisphere have been an important reason for the decline in vegetation cover in some high-latitude regions, and a decline in vegetation cover will lead to a deterioration in the regional ecosystem [3]. In addition to climate changes, human activity can affect regional vegetation coverage [4]. Human behavior can impact the vegetation ecological environment in positive and negative ways. For example, afforestation is a positive impact and improves the quality of the ecological environment [5]. Some negative impacts are that deforestation and land reclamation, which aggravate ecological environment deterioration [6,7]. To restore vegetation and improve the vegetation ecological environment, the Chinese government has implemented numerous measures, among which, the largest and most well-known is the Grain for Green Program (GGP) [8], which includes two aspects: returning sloping farmland to forest and afforestation of barren hills and wasteland suitable for forestry [9]. The geographical scope of the GGP includes the alpine grassland and meadow areas at the source of the Yellow River, the loess hilly and gully areas, and the arid and semi-arid areas of northern China [10]. In such a scenario, understanding the dynamics and attribution of regional vegetation cover and land use can help one garner essential information for vegetation-related planning [11].

The relevant information is particularly critical in arid climates, where vegetation is highly susceptible to water and energy input [12].

The Yellow River Basin (YRB), the second-largest basin in China, has a fragile ecosystem and faces severe environmental challenges [2,4]. The YRB climate region is mainly divided into arid, semi-arid, and semi-humid climate regions, and the dominant land use types are cultivated land, woodland, and grassland [5,7–9]. Owing to severe drought and land desertification, the YRB was selected as a pilot for the GGP in 1999 [12]. Focusing on the conversion of mountainous, hilly, and steep farmland and cultivated land with a slope of more than 6° to woodland and grassland, the GGP has caused great changes in the spatial–temporal characteristics of vegetation cover and land use in the YRB [13]. The GGP, which represents human activities, has had both positive and negative impacts on the YRB. For example, the GGP enhanced watershed climate change; eliminated soil erosion to a certain extent; and increased soil organic carbon storage, which has had a positive influence on soil nutrient circulation and soil moisture storage [14]. However, excessive and unreasonable vegetation planting will aggravate the regional water evaporation and reduce the runoff, leading to drought and other problems [15]. Many past studies have focused on the changes in and impacts of vegetation cover and land use in the YRB, but some issues remain unclear. What are the impacts of climate changes and human activities on the vegetation cover change in the YRB, and how can we quantify them?

Various factors determine vegetation spatial distribution patterns [16]. The water and the material energy required by vegetation determine the large-scale spatial changes in vegetation, while altitude and slope greatly affect the small-scale spatial pattern of vegetation [16,17]. Different altitudes and slopes are suitable for different vegetation types. For example, the elevations and slopes of farmlands are lower and smaller, while those of forests and grasslands are higher and greater [16–18]. Furthermore, the transformation of vegetation types is different at different elevations and slopes. For example, woodlands and grasslands are mainly transformed into each other at high elevations and in great-slope areas. In contrast, construction areas and farmlands are converted to low-altitude and small-slope areas [18–20]. In particular, GGP implementation is closely related to topographic factors. For example, for farmlands located at high altitudes, i.e., on hills and slopes greater than 20°, the GGP requires them to be returned to grasslands and forests [21]. Therefore, when discussing vegetation cover and land use changes in the YRB, considering topographic elements may provide new ideas.

To quantitatively determine the vegetation cover and land use in the YRB, the key is to determine the relationship between vegetation and climate changes to reconstruct the vegetation sequence under natural conditions. For this study, it is critical to identify the long-term vegetation cover sequence on the basis of topographic factors. Currently, the normal difference vegetation index (NDVI) is commonly used to study vegetation coverage [22,23]. The Advanced Very High Resolution Radiometer (AVHRR) NDVI has a long time-series, whereas the SOPTVEGETATION (VGT) NDVI and the Moderate Resolution Imaging Spectroradiometer (MODIS) NDVI have a higher spatial resolution. Since this research requires long-term NDVI datasets (1982–2019), it is essential to integrate and unify NDVI series datasets and generate a long-term and consistent NDVI dataset for research based on having different NDVI data products [24].

The considerable changes in vegetation cover and land use in the YRB induced by the GGP provide the possibility for us to study the correlation and interactions between vegetation cover, climate changes, and human activities. Using the integrated NDVI long time-series, the study aims to achieve the following: (i) use assimilated long-term NDVI data series to assess the spatial–temporal changes in the vegetation cover in the YRB from 1982 to 2019, (ii) analyze the vegetation cover trend and land use changes by using terrain factors, and (iii) quantify the effects of climate changes and human activities on vegetation coverage and land use in the YRB.

## 2. Materials and Methods

### *2.1. Study Area*

The YRB, located between 96–119°E and 32–42°N, with a basin area of 752,443 km$^2$, is the second-largest basin in China (Figure 1a) [6]. The maximum altitude and slope can reach 6009 m and 70.47°, respectively (Figure 1b,c). The YRB is one of the main climate-sensitive areas in China. The mean annual precipitation varies between 166 and 888 mm, and the mean annual temperature ranges from −3.5 to 15 °C. Overall, from the northwest to the southeast, the transition is gradual from dry to wet and the temperature increases from the west to the east (Figure 1d,e) [25]. The NDVI and the vegetation coverage index decrease from the south to the north (Figure 1f). From the east to the west, the YRB spans four vegetation belts: deciduous broad-leaved forest belts, grassland belts, desert belts, and Qinghai–Tibet Plateau vegetation belts. The development of the GGP has led to various ecological construction projects, such as the Three-North Shelterbelt, the Yellow River Middle Reaches Shelter Forest, and Taihang Mountain Greening [26].

We selected 14 sub-basins of the YRB and collected relevant basic data, covering the ages of various climatic, topographic, and NDVI conditions. The upstream and downstream hydrological stations were used as control points in the reaches of a part of the river basin, and these were named and numbered as follows: Upper Yellow River Basin (UYRB): 1–4; Middle Yellow River Basin (MYRB): 5–12; and Lower Yellow River Basin (LYRB): 13–14 (Table 1 and Figure 1a). Due to their distinctive characteristics, the various sub-basins are suitable for vegetation coverage analysis.

### *2.2. Data Source and Processing*

Commonly, there are two NDVI datasets: GIMMS NDVI3g datasets from NASA (http://ecocast.arc.nasa.gov/data/pub/gimms/ (accessed on 22 June 2022)) and the MODIS NDVI from the Resource and Environmental Science and Data Center of the Chinese Academy of Sciences (https://www.resdc.cn/data (accessed on 24 June 2022)). The former has a long monitoring period (1982 to 2015), with a temporal resolution of 15 days and a spatial resolution of 8 km. Although the latter has a higher resolution, the time span is insufficient to support this study. Therefore, first, we preprocessed the two dataset series using monthly maximum value synthesis (MVC), projection grid conversion, clipping, and resampling in ArcGIS 10.5. Then, we performed a correlation analysis on them and the results showed a good linear relationship between 1998 and 2015 (Figure 2a). Comparing the two datasets, it can be observed that the GIMMS NDVI value is greater than the MODIS NDVI value (Figure 2b). Owing to a good linear relationship, we adjusted the MODIS NDVI from 2016–2019 and fused it with the GIMMS NDVI from 1982–2015. Thus, we generated a new NDVI dataset for the period 1982–2019. We then assimilated each raster using ArcGIS 10.5. We used the new NDVI dataset for the study after observing that they have higher values than the MODIS NDVI (Figure 2c).

The preprocessing of meteorological data mainly includes interpolation of missing datasets and null datasets. Meteorological data were obtained from the China Meteorological Science Data Sharing Service Network (http://data.cma.cn/ (accessed on 1 July 2022)), and temperature and precipitation data from 157 weather stations in and around the YRB were selected for the same period (1982–2019) (Figure 1a). The missing data were then interpolated according to the linear interpolation method and the data of adjacent years [27]. The number of missing data only accounts for 0.5% of all data observed from meteorological station with missing conditions, and its impact on the analysis results is negligible [27,28]. Finally, the Kriging interpolation method of the ArcGIS 10.2 spatial analysis module was used to spatially interpolate the annual temperature and precipitation data of the YRB and resample them to a resolution of 8 km. To assess the vegetation spatial pattern variations, elevation and slope were used as topographical factors and their digital elevation model was obtained by using images from the Advanced Spaceborne Thermal Emission and Reflection Radiometer (ASTER) Global Digital Elevation Model (GDEM) with a resolution of 30 m [29,30].

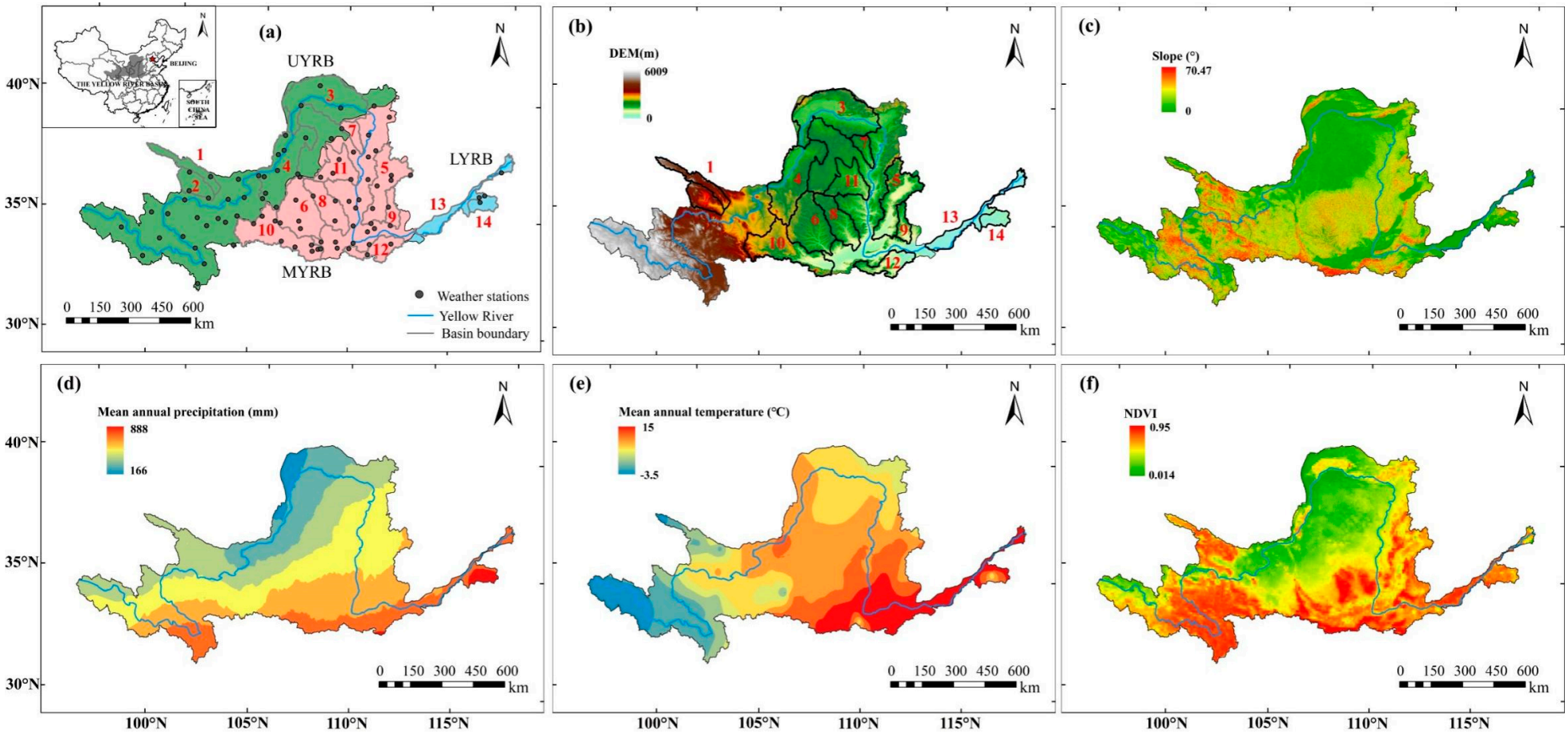


**Figure 1.** Topography of the Yellow River Basin and the spatial pattern of basic elements. (**a**) Geographical location, among which the UYRB, the MYRB, and the LYRB represent Upper Yellow River Basin, Middle Yellow River Basin, and Lower Yellow River Basin, respectively. Red numbers represent selected sub-basins. (**b**) Elevations (m), (**c**) slopes (°), (**d**) mean annual precipitation (mm), (**e**) mean annual temperature (°C), and (**f**) multi-year mean annual NDVI.

**Table 1.** Overview of 14 sub-basins in terms of climate, hydrology, and vegetation from 1982–2019.

| Region | Number | Name | Area ($\times 10^4$ km$^2$) | Elevation (m) | Precipitation (mm/a) | Temperature (°C) | NDVI | Mean Slope (°) |
|---|---|---|---|---|---|---|---|---|
| UYRB | 1 | Datong | 1.44 | 3765.25 | 345.84 | 2.54 | 0.68 | 13.34 |
| | 2 | HuangShui | 1.55 | 3642.61 | 375.32 | 4.43 | 0.66 | 13.26 |
| | 3 | Shizuishan-Toudaoguai | 7.08 | 1476 | 259.21 | 7.26 | 0.30 | 3.15 |
| | 4 | Xiaheyan-Shizuishan | 5.45 | 1729.37 | 265.54 | 9.08 | 0.30 | 3.71 |
| MYRB | 5 | Fen | 3.88 | 1509.46 | 486.09 | 10.43 | 0.64 | 8.46 |
| | 6 | Jing | 4.29 | 1707.21 | 491.63 | 9.36 | 0.53 | 11.44 |
| | 7 | Kuye | 0.90 | 1320.78 | 401.00 | 8.05 | 0.36 | 4.79 |
| | 8 | Beiluo | 2.62 | 1370.16 | 499.48 | 9.93 | 0.68 | 11.39 |
| | 9 | Qin | 0.91 | 1329.76 | 535.84 | 10.51 | 0.74 | 10.31 |
| | 10 | Wei | 4.54 | 1980.07 | 532.99 | 8.56 | 0.64 | 12.22 |
| | 11 | Wuding | 2.41 | 1317.47 | 417.24 | 9.14 | 0.37 | 6.03 |
| | 12 | Yiluo | 1.73 | 1043.85 | 648.15 | 12.93 | 0.75 | 10.42 |
| LYRB | 13 | Gaocun-Lijin | 2.19 | 69.52 | 631.36 | 13.87 | 0.66 | 1.23 |
| | 14 | Upper daicunba | 0.84 | 300.06 | 725.79 | 10.89 | 0.69 | 3.88 |

UYRB: Upper Yellow River Basin; MYRB: Middle Yellow River Basin; LYRB: Lower Yellow River Basin; NDVI: normal difference vegetation index. For individual sub-basins, the upstream and downstream hydrological stations, such as Shizuishan-Toudaoguai. Areas numbered 1–14 represent the corresponding sub-basins. NDVI is the mean annual NDVI.

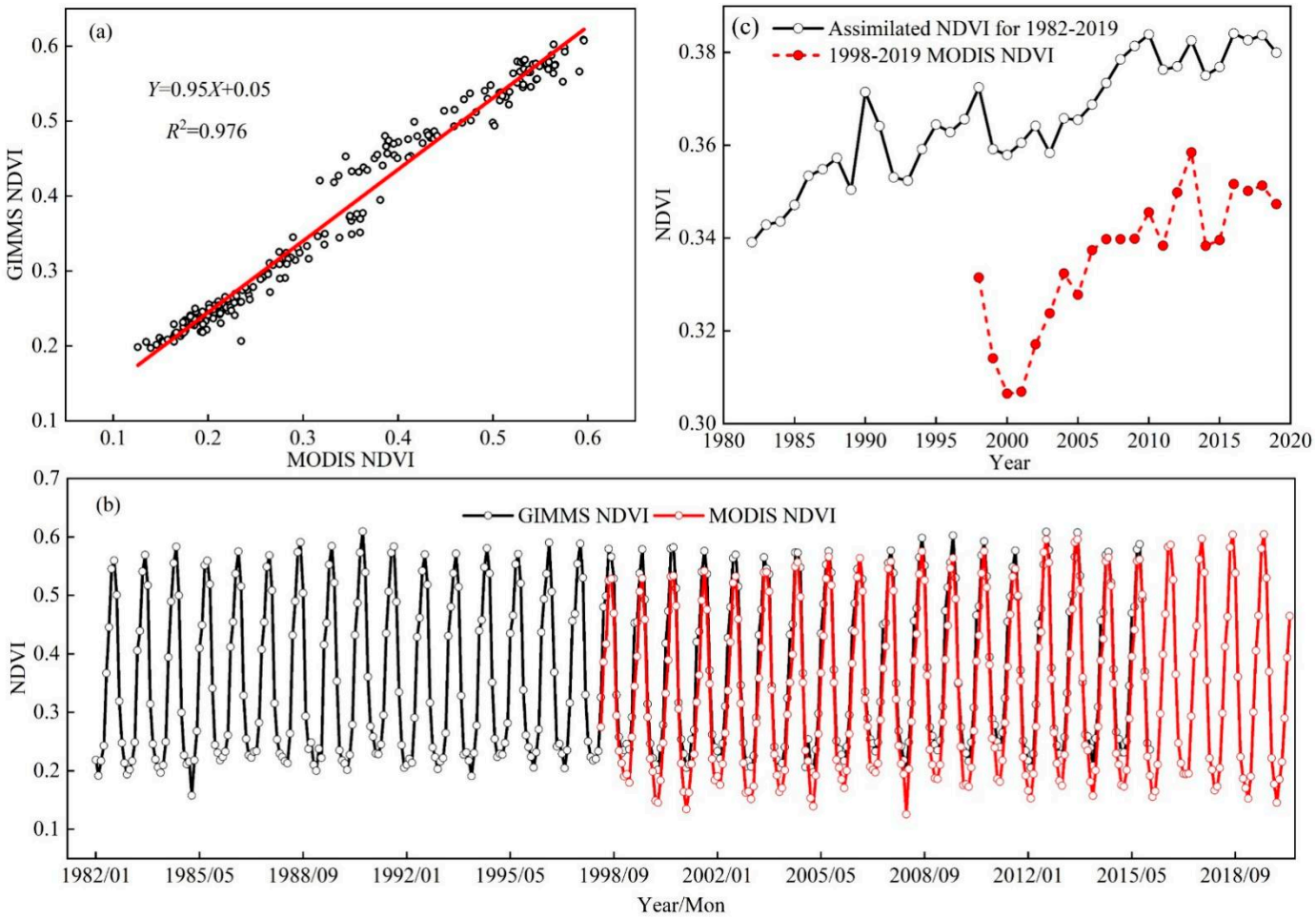


**Figure 2.** NDVI data preprocessing. (**a**) Correlation analysis between the GIMMS NDVI and the MODIS NDVI, (**b**) comparison of the GIMMS NDVI and the MODIS NDVI data sequences, and (**c**) comparison of assimilated NDVI and MODIS NDVI data. NDVI: normal difference vegetation index.

### *2.3. Methods*

#### 2.3.1. Spatial–Temporal Variations in NDVI

On the basis of different vegetation levels represented by different NDVIs, the NDVI was divided into five types: $L_1$ (0.0–0.2), $L_2$ (0.2–0.4), $L_3$ (0.4–0.6), $L_4$ (0.6–0.8), and $L_5$ (0.8–1.0) [29]. NDVI spatial–temporal analysis was undertaken using variation magnitude, speed, and type. The variation magnitude is the difference between the beginning and the end of the NDVI, the variation speed represents the slope of a linear fit over a period, and the variation type is the conversion of an NDVI level.

Furthermore, to analyze the NDVI spatial variation, we introduced the topographic elements of elevation and slope. The five levels of NDVI at different altitudes and slopes were calculated using histograms, and the overall NDVI spatial characteristics in the YRB were determined. The YRB elevations are divided into six categories: <800, 800–1200, 1200–1600, 1600–2000, 2000–2500, and >2500 m. Their area ratios are, respectively, 12%, 18.5%, 28%, 10.7%, 5.2%, and 25.6%. Slopes were divided into three types, i.e., <10°, 10–20°, >20°, according to the critical gradient determined by the GGP, and the areas account for 40%, 53.2%, and 6.8% of the total area, respectively.

#### 2.3.2. Vegetation Attribution Analysis

As mentioned in the introduction, in order to quantitatively analyze the changes in the vegetation cover of the YRB, we conducted research from two aspects: climate change

(CC) and human activities (HA). The key to analyzing these two aspects is to calculate their contribution rates separately.

First, in a given area, we select a period of time scale $t$ for research. The annual average NDVI has a specific value in this time scale, $\overline{NDVI}_t$, which can be decomposed into climate change ($\overline{NDVI}_{CC,t}$) and human activities ($\overline{NDVI}_{HA,t}$):

$$\overline{NDVI}_t = \overline{NDVI}_{CC,t} + \overline{NDVI}_{HA,t} \quad (1)$$

Then, if there are great variations in HAs in different periods, the study period $t$ can be divided into two sub-periods: $t_1$ (before change) and $t_2$ (after change). Generally, there is little human activity (HA) during $t_1$ (before change). Therefore, the NDVI has a good correlation with climate factors, such as precipitation and temperature, in $t_1$. Therefore, over $t_1$, Equation (1) can be expressed as:

$$\overline{NDVI}_{t_1} = f(CC_{t_1}) + \overline{NDVI}_{HA,t_1} \quad (2)$$

where $f(CC_{t_1})$ is the NDVI value estimated by linear fitting of climate and the NDVI and $\overline{NDVI}_{HA,t_1}$ is the average NDVI induced by human activities during $t_1$, which is the residual between the observed mean value and the fitted mean value of linear fitting, that is, $\overline{NDVI}_{HA,t_1}$ and $f(CC_{t_1})$.

With considerable human activities (HA) over period $t_2$ (after change), the relationship $f(CC_{t_1})$ between the NDVI and climate obtained by Equation (2) can be used in $t_2$ to calculate the NDVI sequence only under the influence of climate conditions, i.e., $\overline{NDVI}_{cal,t_2}$. Then, combined with the annual mean observation value of the NDVI in $t_2$ ($\overline{NDVI}_{obs,t_2}$), those induced by HA in $t_2$, that is, $\overline{NDVI}_{HA,t_2}$, are calculated:

$$\overline{NDVI}_{HA,t_2} = \overline{NDVI}_{obs,t_2} - \overline{NDVI}_{cal,t_2} \quad (3)$$

where $\overline{NDVI}_{obs,t_2}$ and $\overline{NDVI}_{cal,t_2}$ are, respectively, observed and calculated average NDVI sequences.

The annual mean NDVI has a specific amount of change from $t_1$ (before change) to $t_2$ (after change), i.e., $\Delta\overline{NDVI}_{tot}$. $\Delta\overline{NDVI}_{tot}$ can be calculated as:

$$\Delta\overline{NDVI}_{tot} = \overline{NDVI}_{t_2} - \overline{NDVI}_{t_1} \quad (4)$$

After calculating $\Delta\overline{NDVI}_{tot}$ according to Equation (4), based on Equation (1), $\Delta\overline{NDVI}_{tot}$ can be decomposed into changes in climate change ($\Delta\overline{NDVI}_{CC}$) and human activities ($\Delta\overline{NDVI}_{HA}$):

$$\Delta\overline{NDVI}_{tot} = \Delta\overline{NDVI}_{CC} + \Delta\overline{NDVI}_{HA} \quad (5)$$

On the basis of Equations (1)–(3), $\Delta\overline{NDVI}_{CC}$ and $\Delta\overline{NDVI}_{HA}$ can be written with the corresponding values estimated over $t_1$ and $t_2$ as follows:

$$\Delta\overline{NDVI}_{CC} = \Delta\overline{NDVI}_{CC,t_2} - \Delta\overline{NDVI}_{CC,t_1} \quad (6)$$

$$\Delta\overline{NDVI}_{HA} = \Delta\overline{NDVI}_{HA,t_2} - \Delta\overline{NDVI}_{HA,t_1} \quad (7)$$

Therefore, the contribution rate can be calculated as the proportion of $\Delta\overline{NDVI}_{CC}$ and $\Delta\overline{NDVI}_{HA}$ in $\Delta\overline{NDVI}_{tot}$, i.e., $\frac{\Delta\overline{NDVI}_{CC}}{\Delta\overline{NDVI}_{tot}}$ and $\frac{\Delta\overline{NDVI}_{HA}}{\Delta\overline{NDVI}_{tot}}$. They, respectively, represent the impacts of climate changes and human activities on vegetation coverage.

The above is the entire quantitative vegetation analysis process, in which Equations (2) and (5) are the more important formulas. The former is the key to reconstructing the NDVI sequence under natural conditions, while the latter is a necessary step to calculate the contribution rate of climate change (CC) and human activities (HA). Since the GGP began in 1999, we divided the 1982–2019 study period into two sub-periods: $t_1$ (1982–1999) and $t_2$ (2000–2019). The discussion of the vegetation coverage conditions in the YRB is based on these sub-periods.

## 3. Results

### *3.1. Overall Characteristics of the Vegetation Cover in the YRB*

The YRB multi-year annual mean NDVIs were 0.51 and 0.58, respectively, representing the GGP before (1982–1999) and after startup (2000–2019), and the sub-basin multi-year annual mean NDVIs ranged from 0.28 to 0.75 and 0.35 to 0.78, respectively (Table 2). More than 78% of the sub-watersheds had a significant ($p < 0.01$) NDVI variation rate after the GGP started, indicating a visibly positive impact of the GGP on vegetation cover change in the YRB. Vegetation coverage for most areas of the YRB was within $L_2$ (0.2–0.4), $L_3$ (0.4–0.6), and $L_4$ (0.6–0.8), with area percentages of 27.7%, 22.6%, and 24.7%, respectively (Figure 3a and Table 3). This implies that main land use and vegetation cover types in the YRB are farmlands, grasslands, and forests.

Combining Figures 1b,f and 3a, the NDVI gradually decreases with an increase in altitude (from southeast to northwest). Figure 3a shows that higher NDVI levels ($L_4$–$L_5$) are distributed in the UYRB at high altitudes (>2500 m). The areas with 200–400 mm of precipitation all year round have low NDVI levels ($L_1$–$L_2$). Conversely, mid/high NDVI levels ($L_3$–$L_5$) tend to be distributed in areas with higher rainfall intensities (400–800 mm) (Figure 3b). Areas with moderate temperatures (3–11 °C) have mainly low NDVI levels, with an area ratio of 29%, i.e., more than 10 times that at other temperatures (area ratio of 2%) (Table 3). In contrast, mid/high NDVI levels seem to be less sensitive to temperature and are distributed more evenly across different temperature gradients. Vegetation coverage is also closely related to slope, with more than 65% of the NDVI located in areas with a slope < 10°, 25.6% located in areas with a slope of 10–20°, and 8.8% located in areas with a slope > 20° (Figure 3d).

### *3.2. Temporal Features of the Vegetation in the YRB*

Significant NDVI variations ($p < 0.05$ and $p < 0.01$) were observed in the YRB before and after GGP initiation (Figure 4a). The latter changed six times quicker than the former, and in general, the NDVI of the YRB showed an upward trend during the entire study period. The NDVI variation trends in the UYRB and MYRB sub-basins were similar to that in the YRB but fluctuated remarkably in the LYRB (Figure 4b–d). The speed of change was not remarkable in the sub-basins of the LYRB as compared that in sub-basins of the UYRB and the MYRB. Most of the UYRB and MYRB sub-basins had a clear change speed rate after the start of the GGP, and in some cases, it was 10 times more than before the start of the GGP (Table 2). The YRB and sub-basin NDVI change speed in the three periods can be spatially displayed. The change in the vegetation coverage in the northeast of the YRB was clear over 1982–1999 but was not clear or showed a negative growth in most other areas (Figure 5a). However, many areas in the MYRB showed a remarkable NDVI growth trend (Figure 5b) in the same period due to GGP initiation during that period (2000–2019) (Figure 5c).

**Table 2.** Mean value of, the magnitude of change in, and the speed of change in the YRB and sub-basins in three periods.

| Region | | Mean | | | Variation Magnitude | | | Variation Speed ($a^{-1}$) | | |
|---|---|---|---|---|---|---|---|---|---|---|
| Year | | 1982–1999 | 2000–2019 | 1982–2019 | 1982–1999 | 2000–2019 | 1982–2019 | 1982–1999 | 2000–2019 | 1982–2019 |
| YRB | | 0.5105 | 0.5795 | 0.556 | 0.0248 | 0.1161 | 0.1427 | 0.0011 * | 0.0067 ** | 0.0027 ** |
| UYRB | 1 | 0.6633 | 0.6967 | 0.68 | 0.0197 | 0.0619 | 0.0786 | 0.0006 | 0.0041 ** | 0.0013 ** |
| | 2 | 0.6563 | 0.6996 | 0.6779 | 0.0322 | 0.0997 | 0.121 | 0.0009 | 0.0055 ** | 0.0017 ** |
| | 3 | 0.2764 | 0.3509 | 0.3137 | 0.0406 | 0.0954 | 0.144 | 0.0020 ** | 0.0062 ** | 0.0028 ** |
| | 4 | 0.2757 | 0.3679 | 0.3218 | 0.0451 | 0.1628 | 0.2033 | 0.0015 * | 0.0088 ** | 0.0036 ** |
| MYRB | 5 | 0.5984 | 0.6945 | 0.6465 | −0.0152 | 0.1386 | 0.1451 | 0.0002 | 0.0087 ** | 0.0037 ** |
| | 6 | 0.4976 | 0.6003 | 0.5489 | 0.0324 | 0.1957 | 0.2304 | 0.0008 | 0.0105 ** | 0.0042 ** |
| | 7 | 0.3175 | 0.4447 | 0.3811 | −0.0233 | 0.1837 | 0.2363 | 0.0025 ** | 0.0107 ** | 0.0051 ** |
| | 8 | 0.6529 | 0.7208 | 0.6869 | 0.0105 | 0.1193 | 0.1259 | 0.0007 | 0.0067 ** | 0.0027 ** |
| | 9 | 0.7033 | 0.7801 | 0.7417 | 0.0283 | 0.0952 | 0.1017 | 0.0006 | 0.0056 ** | 0.0029 ** |
| | 10 | 0.6384 | 0.6948 | 0.6666 | 0.0404 | 0.1426 | 0.1588 | 0.0003 | 0.0070 ** | 0.0024 ** |
| | 11 | 0.3258 | 0.4658 | 0.3958 | 0.0156 | 0.1776 | 0.2187 | 0.0016 | 0.0112 ** | 0.0057 |
| | 12 | 0.7462 | 0.775 | 0.7606 | 0.0197 | 0.0428 | 0.0701 | 0.0006 | 0.0018 | 0.0010 ** |
| LYRB | 13 | 0.7285 | 0.7457 | 0.7371 | 0.0772 | 0.004 | 0.078 | 0.0022 | 0.0007 | 0.0008 |
| | 14 | 0.6894 | 0.7132 | 0.7013 | 0.0534 | 0.0285 | 0.1012 | 0.0027 * | 0.0017 | 0.0009 |

* represents significance ($p < 0.05$), ** represents extreme significance ($p < 0.01$), and others are not significant ($p > 0.05$). The sub-basins represented by numbers 1–14 are Datong, Huangshui, Shizuishan-Toudaoguai, Xiaheyan-Shizuishan, Fen, Jing, Kuye, Beiluo, Qin, Wei, Wuding, Yiluo, Gaocun-Lijin, and Upper daicunba.

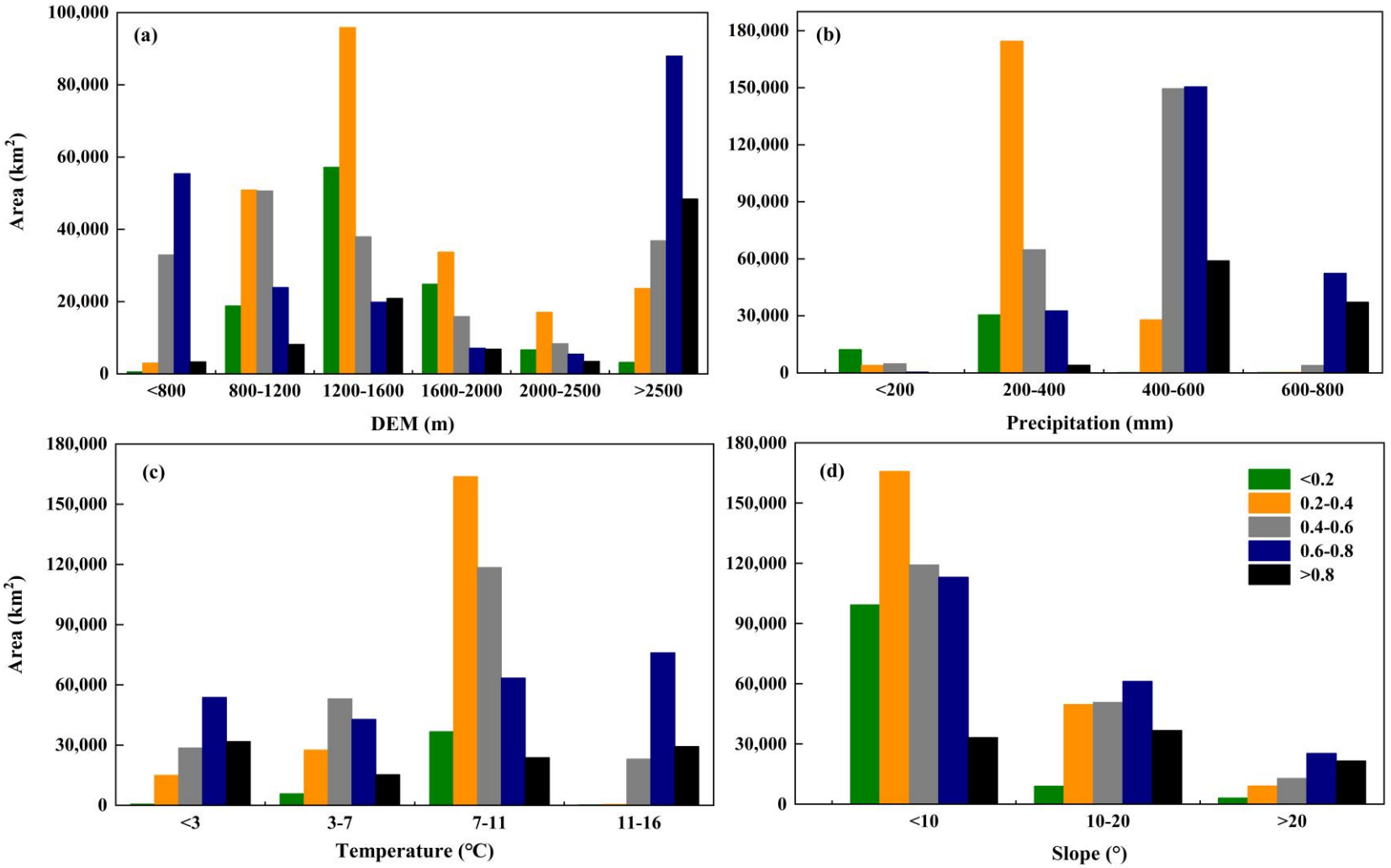


**Figure 3.** Distribution of different levels of the normal difference vegetation index (NDVI) under different types of topographic and climatic factors. (**a**) Elevations (m), (**b**) precipitation (mm), (**c**) temperature (°C), and (**d**) slope (°). In the legend, <0.2, 0.2–0.4, 0.4–0.6, 0.6–0.8, and >0.8 represent NDVI levels $L_1$, $L_2$, $L_3$, $L_4$, and $L_5$, respectively.

**Table 3.** Area ratios of all NDVI levels under different influencing factors.

| | | Influence Factors Area Rate (%) | | | | |
|---|---|---|---|---|---|---|
| | | $L_1$ | $L_2$ | $L_3$ | $L_4$ | $L_5$ |
| DEM (m) | <800 | 0.08 | 0.37 | 4.07 | 6.84 | 0.41 |
| | 800–1200 | 2.33 | 6.29 | 6.26 | 2.96 | 1.01 |
| | 1200–1600 | 7.06 | 11.84 | 4.69 | 2.46 | 2.58 |
| | 1600–2000 | 3.07 | 4.17 | 1.96 | 0.88 | 0.85 |
| | 2000–2500 | 0.82 | 2.11 | 1.04 | 0.68 | 0.43 |
| | >2500 | 0.40 | 2.92 | 4.56 | 10.86 | 5.98 |
| Precipitation (mm) | <200 | 1.52 | 0.49 | 0.60 | 0.06 | 0.00 |
| | 200–400 | 3.78 | 21.56 | 8.02 | 4.03 | 0.50 |
| | 400–600 | 0.03 | 3.45 | 18.47 | 18.59 | 7.28 |
| | 600–800 | 0.03 | 0.04 | 0.49 | 6.47 | 4.60 |
| Temperature (°C) | <3 | 0.08 | 1.85 | 3.53 | 6.64 | 3.93 |
| | 3–7 | 0.72 | 3.40 | 6.56 | 5.30 | 1.88 |
| | 7–11 | 4.54 | 20.23 | 14.63 | 7.83 | 2.94 |
| | 11–16 | 0.03 | 0.06 | 2.85 | 9.39 | 3.62 |
| Slope (°) | <10 | 12.26 | 20.48 | 14.73 | 13.97 | 4.10 |
| | 10–20 | 1.10 | 6.13 | 6.27 | 7.56 | 4.53 |
| | >20 | 0.38 | 1.12 | 1.58 | 3.13 | 2.66 |

Area ratios of all normal difference vegetation index (NDVI) levels under different influencing factors. $L_1$–$L_5$ represent the following NDVI levels, respectively: <0.2, 0.2–0.4, 0.4–0.6, 0.6–0.8, and >0.8. DEM: digital elevation model.

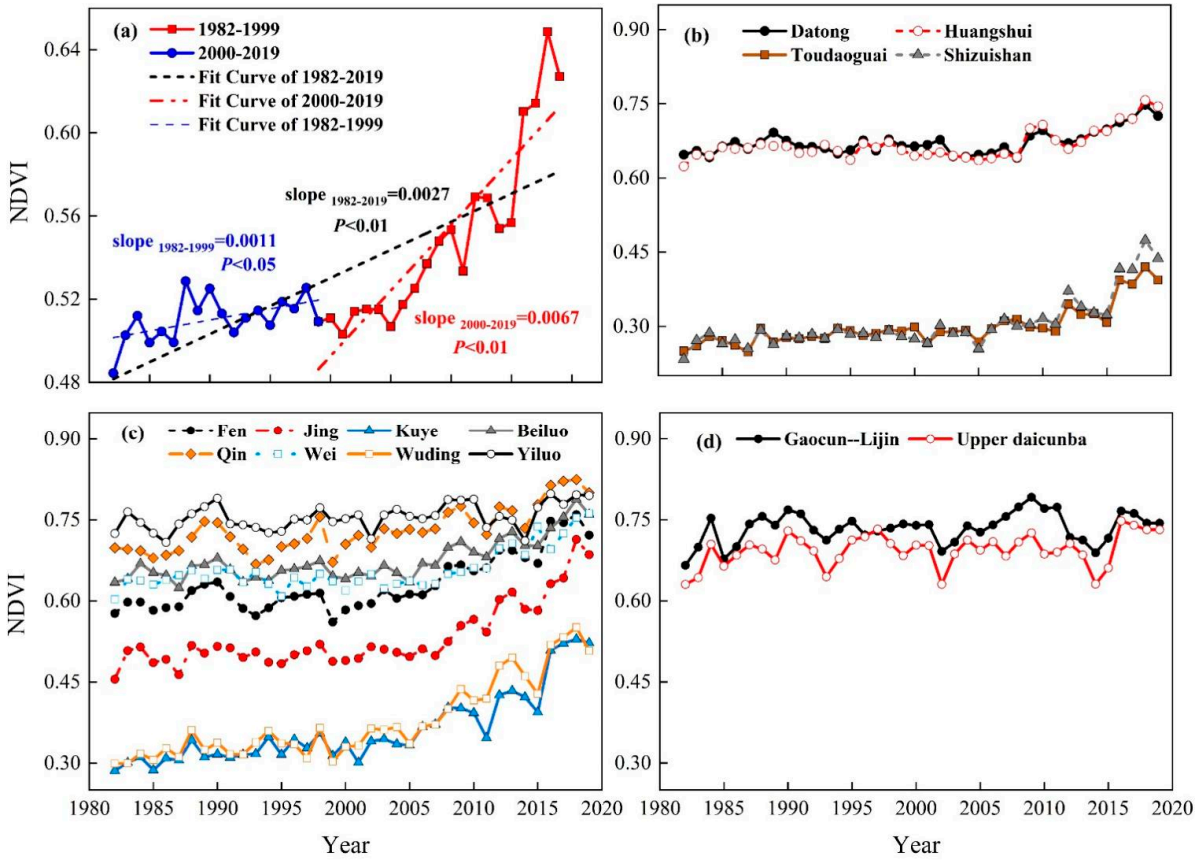


**Figure 4.** Temporal variation in the NDVI levels in the YRB and sub-basins. (**a**) Temporal variation in the NDVI levels in the YRB from 1982 to 2019 and two sub-periods, (**b**) four sub-basins in the UYRB, (**c**) eight sub-basins in the MYRB, and (**d**) two sub-basins in the LYRB. NDVI: normal difference vegetation index; YRB: Yellow River Basin; UYRB: Upper Yellow River Basin; MYRB: Middle Yellow River Basin; LYRB: Lower Yellow River Basin.

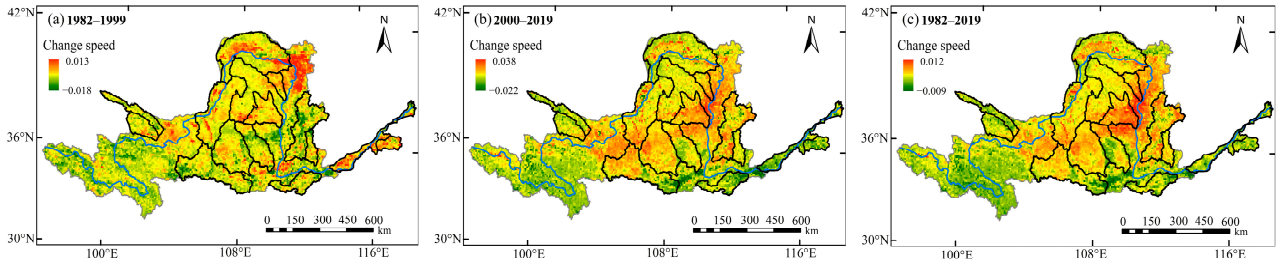


**Figure 5.** Spatial change speed patterns of three periods in the Yellow River Basin (YRB). Change speed: slope of linear fit over a period of time.

From the observations, in the YRB, low NDVI levels ($L_1$–$L_2$) were converted to high NDVI levels ($L_4$–$L_5$), quantitatively, and the low-level NDVI area decreased by 25.2% and the high-level NDVI area increased by 25.14% (Figure 6). However, the temporal variation in all NDVI levels in each sub-basin varied. In the UYRB, the areas shown in Figure 7a,b changed from high-level NDVIs to high-level NDVIs ($L_4$–$L_5$), while for the areas shown in Figure 7c,d, low-level NDVIs converted to medium-level and high-level NDVIs ($L_1$ to $L_3$ and $L_4$) (Figure 7a–d). The MYRB NDVIs were all at medium–high levels: In the eight sub-basins, there were almost 0 $L_1$ areas, and $L_2$ areas changed to high levels. Except for the areas displayed in Figure 7g,k, the $L_5$ areas in the other sub-basins increased, and after the year 2000 (after the initiation of the GGP), $L_3$ transformed to $L_4$ and $L_5$, accounting for the majority of the areas (Figure 7e–l). In the LYRB, the variation in the area shown in Figure 7m in the NDVI was relatively stable and the $L_4$ area was the largest, while the NDVI levels of the area shown in Figure 7n were basically $L_4$ and $L_5$, and its change rule was not considerable and fluctuated greatly (Figure 7m,n). Most of the sub-basins in the MYRB had the same NDVI variation trend as that in the YRB, and the variation in the 2000–2019 sub-period was greater than that in 1982–1999.

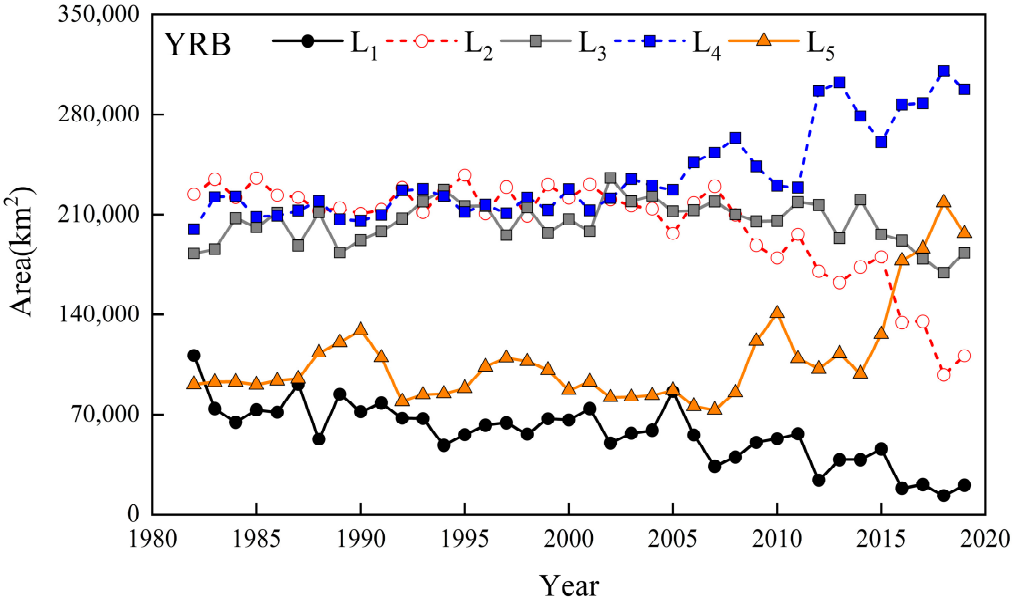


**Figure 6.** Temporal variation in the normal difference vegetation index (NDVI) at all levels in the Yellow River Basin (YRB). $L_1$–$L_5$ represent NDVI levels of <0.2, 0.2–0.4, 0.4–0.6, 0.6–0.8, and >0.8 respectively.

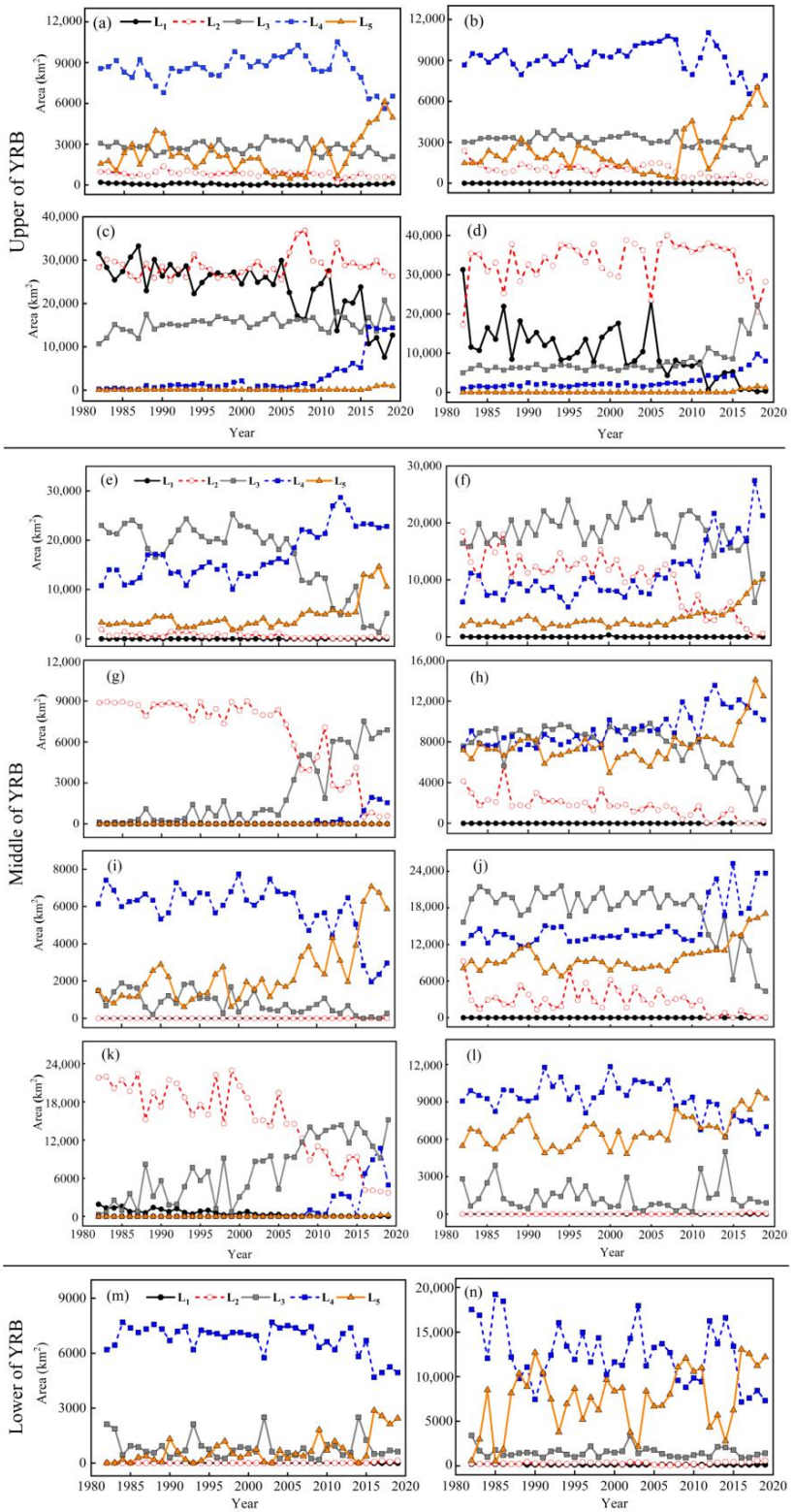


**Figure 7.** Temporal variation in the normal difference vegetation index (NDVI) at all levels in the sub-basins of the Yellow River Basin (YRB). $L_1$–$L_5$ represent the NDVI levels of <0.2, 0.2–0.4, 0.4–0.6, 0.6–0.8, and >0.8, respectively. (**a**–**d**) represent Datong, Huangshui, Shizuishan-Toudaoguai, and Xiaheyan-Shizuishan in the Upper Yellow River Basin, respectively; (**e**–**l**) represent Fen, Jing, Kuye, Beiluo, Qin, Wei, Wuding, and Yiluo in the Middle Yellow River Basin, respectively; and (**m**,**n**) represent Gaocun-Lijin and Upper daicunba, respectively.

### *3.3. Spatial Variation in Vegetation in the YRB*

Spatial patterns of the two sub-periods (1982–1999 and 2000–2019) in the YRB were similar to that of the entire period (1982–2019), and NDVI levels increased from the northwest to the east and the south (Figure 8a–c). From the observations, it can be seen that during 2000–2019, when human activities were prevalent, NDVI levels in the southeast of the YRB considerably increased and the low-level NDVI area in the northwest remarkably decreased when compared with that in 1982–1999.

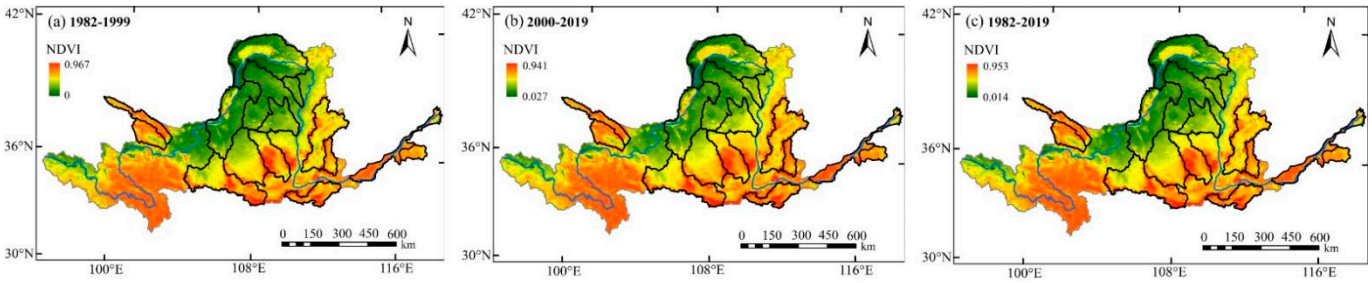


**Figure 8.** Spatial patterns of the normal difference vegetation index (NDVI) in different time periods in the Yellow River Basin (YRB). (**a**) 1982–1999, (**b**) 2000–2019, and (**c**) 1982–2019.

The spatial patterns of all levels of NDVI were further analyzed and calculated (Figure 9a,b). The distribution characteristics of all NDVI levels in terms of elevation and slope were similar. A high-level NDVI was more inclined to high-elevation and steep-slope areas, whereas a low-level NDVI was inclined to low-elevation and shallow-slope areas. The average elevation level of a high-level NDVI ($L_4$ and $L_5$) fluctuated greatly, but slope inclinations were relatively stable (Figure 9a,b). Further observation showed that the average elevation of $L_5$ reached a historical minimum in 2008, which appears to be an outlier. The reason for this may be that in 2008, GGP activity reached an all-time high, as more low-elevation farmlands were converted to forests and more forests were planted in low-elevation areas. However, in the time period that followed, $L_5$ moved to high-altitude areas, possibly because excessive forest planting led to increased water consumption and evaporation, which made forests unsuitable for living in the new low-altitude areas. We further calculated the average elevation and slope inclinations of all NDVI levels in each sub-basin (Table 4). The NDVI levels in the YRB had different characteristics in the transition from $t_1$ (1982–1999) to $t_2$ (2000–2019). Low-level NDVIs, such as $L_2$ and $L_3$, moved to higher-altitude areas, but high-level NDVIs, such as $L_4$ and $L_5$, moved to lower-altitude areas. However, the slope variations across all NDVI levels were relatively consistent and all moved to shallow-slope areas.

From Table 4, in the UYRB sub-basins (1–4), most NDVI levels show a shift toward low elevations, with a few showing the opposite trend, where the NDVI shifts toward steep-slope areas. The NDVI variation characteristics in the sub-basins of the MYRB (5–12) are similar to those in the sub-basins of the YRB: a low-level NDVI ($L_1$–$L_2$) shifts toward higher elevations, whereas a middle- to high-level NDVI ($L_3$–$L_5$) shifts toward lower elevations, with the majority shifting toward shallow-slope areas. NDVI variations in the LYRB (13–14) are small, but all shift toward high-elevation and steep-slope areas.

### *3.4. Attribution Analysis of NDVI Variation in the YRB*

#### 3.4.1. Qualitative Analysis of the NDVI

Climate change is a major factor that determines vegetation distribution patterns. The input of water and energy to a specific area is crucial for the distribution of vegetation. Therefore, it is necessary to analyze climate and vegetation distribution patterns. Spatial distribution patterns of vegetation in the YRB were consistent with temperature and precipitation: the levels in the east and south were high, while those in the northwest were low (Figure 1d–f), and the temporal variation trend was consistent (Figure 10). In the YRB, vegetation coverage is closely related to climate change and the correlation coefficients

between precipitation and temperature NDVI reached 0.84 and 0.88 ($p < 0.01$), respectively, over $t_1$ (1982–1999) (Figure 11a,b). These results indicate that the spatial distribution pattern of and temporal variation in the NDVI are strongly correlated with precipitation and temperature. Furthermore, from 1982 to 1999, precipitation in the YRB did not change significantly ($p = 0.3$) but temperature rise was extremely significant ($p < 0.01$) and the change in the NDVI in the YRB still increased significantly ($p < 0.05$) (Figures 4a and 11c,d). This shows that although drought and water shortage will have a great impact on vegetation coverage in the Yellow River Basin, temperature can also have a strong positive impact on vegetation coverage at a certain time scale and is a dominant factor.

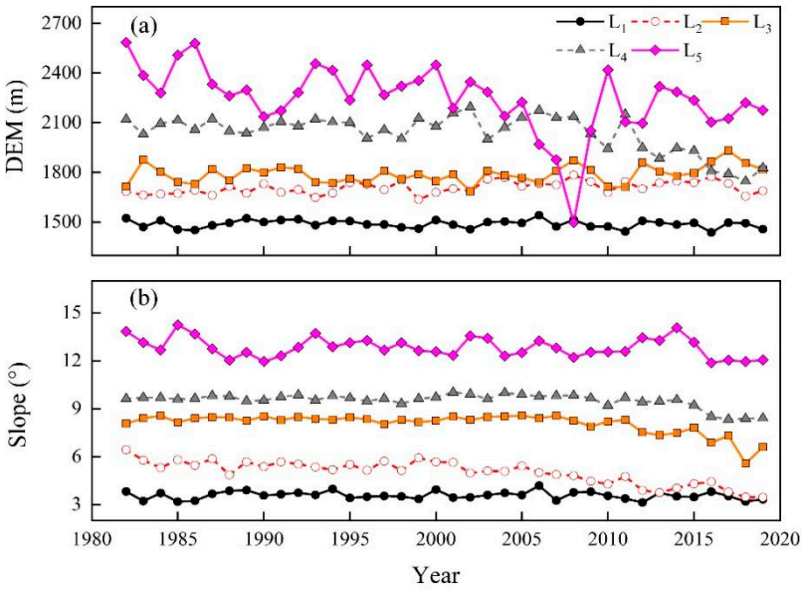


**Figure 9.** Spatial variation (elevation and slope) across all levels of the normal difference vegetation index (NDVI) of the Yellow River Basin (YRB). (**a**) Elevation (m) and (**b**) slope (°). $L_1$–$L_5$ represent the following NDVI levels, respectively: <0.2, 0.2–0.4, 0.4–0.6, 0.6–0.8, and >0.8. DEM: digital elevation model.

**Table 4.** Mean elevation and slope of all levels of NDVI in each sub-basin.

| | District | NDVI Rank | Average Elevation, m | | | Average Slope, ° | | |
|---|---|---|---|---|---|---|---|---|
| | | | 1982–1999 | 2000–2019 | Range | 1982–1999 | 2000–2019 | Range |
| | YRB | L1 | 1490.82 | 1487.17 | −3.65 | 3.58 | 3.57 | −0.01 |
| | | L2 | 1689.92 | 1725.03 | 35.11 | 5.54 | 4.56 | −0.98 |
| | | L3 | 1780.65 | 1797.97 | 17.32 | 8.34 | 7.84 | −0.5 |
| | | L4 | 2078.41 | 2004.45 | −73.96 | 9.64 | 9.42 | −0.22 |
| | | L5 | 2351.64 | 2155.98 | −195.66 | 12.97 | 12.73 | −0.24 |
| UYRB | 1 | L3 | 3753.65 | 3640.40 | −113.25 | 13.21 | 12.97 | −0.24 |
| | | L4 | 3446.90 | 3472.95 | 26.05 | 12.00 | 11.98 | −0.02 |
| | | L5 | 3188.87 | 3168.63 | −20.24 | 17.40 | 17.08 | −0.32 |
| | 2 | L3 | 2612.12 | 2460.09 | −152.03 | 12.39 | 13.72 | 1.33 |
| | | L4 | 3204.76 | 3185.41 | −19.35 | 14.47 | 14.56 | 0.09 |
| | | L5 | 3186.87 | 3218.60 | 31.73 | 12.99 | 14.90 | 1.91 |
| | 3 | L1 | 1414.67 | 1387.73 | −26.94 | 3.59 | 4.56 | 0.97 |
| | | L2 | 1498.14 | 1476.35 | −21.79 | 3.68 | 3.42 | −0.26 |
| | | L3 | 1419.33 | 1477.15 | 57.82 | 4.58 | 4.85 | 0.27 |
| | 4 | L1 | 1263.88 | 1279.97 | 16.09 | 4.12 | 4.82 | 0.70 |
| | | L2 | 1288.97 | 1298.87 | 9.90 | 3.25 | 3.26 | 0.01 |
| | | L3 | 1086.45 | 1101.58 | 15.13 | 1.48 | 1.74 | 0.26 |

**Table 4.** *Cont.*

| | District | NDVI Rank | Average Elevation, m | | | Average Slope, ° | | |
|---|---|---|---|---|---|---|---|---|
| | | | 1982–1999 | 2000–2019 | Range | 1982–1999 | 2000–2019 | Range |
| MYRB | 5 | L3 | 1017.00 | 904.25 | −112.75 | 7.23 | 6.37 | −0.86 |
| | | L4 | 1216.13 | 1153.18 | −62.95 | 9.12 | 8.19 | −0.93 |
| | | L5 | 1654.77 | 1592.02 | −62.75 | 15.71 | 14.98 | −0.73 |
| | 6 | L2 | 1574.07 | 1617.19 | 43.12 | 11.48 | 9.43 | −2.05 |
| | | L3 | 1309.11 | 1426.34 | 117.23 | 10.63 | 11.57 | 0.94 |
| | | L4 | 1425.30 | 1341.13 | −84.17 | 11.99 | 11.02 | −0.97 |
| | | L5 | 1610.86 | 1543.71 | −67.15 | 13.73 | 13.83 | 0.10 |
| | 7 | L2 | 1265.52 | 1321.28 | 55.76 | 5.11 | 4.09 | −1.02 |
| | | L3 | 1277.67 | 1205.84 | −71.83 | 2.46 | 5.97 | 3.51 |
| | 8 | L3 | 1262.94 | 1351.50 | 88.56 | 10.69 | 11.05 | 0.36 |
| | | L4 | 1163.61 | 1145.08 | −18.53 | 11.06 | 10.50 | −0.56 |
| | | L5 | 1366.98 | 1360.90 | −6.08 | 12.01 | 12.05 | 0.04 |
| | 9 | L4 | 1080.30 | 1012.52 | −67.78 | 10.18 | 9.46 | −0.72 |
| | | L5 | 1413.47 | 1290.74 | −122.73 | 15.98 | 13.43 | −2.55 |
| | 10 | L3 | 1763.30 | 1819.40 | 56.10 | 10.60 | 10.74 | 0.14 |
| | | L4 | 1330.74 | 1332.93 | 2.19 | 9.57 | 9.01 | −0.56 |
| | | L5 | 1736.88 | 1740.13 | 3.25 | 19.42 | 19.06 | −0.36 |
| | 11 | L2 | 1234.23 | 1259.98 | 25.75 | 5.64 | 1.93 | −3.71 |
| | | L3 | 1147.33 | 1203.86 | 56.53 | 8.17 | 8.09 | −0.08 |
| | 12 | L4 | 546.46 | 517.02 | −29.44 | 7.07 | 6.12 | −0.95 |
| | | L5 | 1133.45 | 1115.26 | −18.19 | 16.85 | 16.71 | −0.14 |
| LYRB | 13 | L4 | 68.39 | 71.10 | 2.71 | 1.47 | 1.66 | 0.19 |
| | | L5 | 56.47 | 56.57 | 0.10 | 0.40 | 0.41 | 0.01 |
| | 14 | L4 | 201.03 | 203.22 | 2.19 | 3.81 | 3.84 | 0.03 |

$L_1$–$L_5$ represent the following NDVI levels, respectively: <0.2, 0.2–0.4, 0.4–0.6, 0.6–0.8, and >0.8. 1–4 represent Datong, Huangshui, Shizuishan-Toudaoguai, and Xiaheyan-Shizuishan in the Upper Yellow River Basin (UYRB), respectively; 5–12 represent Fen, Jing, Kuye, Beiluo, Qin, Wei, Wuding, and Yiluo in the Middle Yellow River Basin (MYRB), respectively; and 13 and 14 represent Gaocun-Lijin and Upper daicunba in the Lower Yellow River Basin (LYRB), respectively. NDVI: normal difference vegetation index.

In the hypothesis of this study, the factors affecting the vegetation cover in the YRB are climate change and human activities. Figures 4a and 11c,d show that from 2000 to 2019 ($t_2$), the changes in precipitation and temperature in the YRB were not significant ($p = 0.2$ and $p = 0.7$) but the NDVI in the YRB showed a significant upward trend (slope = $6.7 \times 10^{-2}$; $p < 0.01$), indicating that the changes in the NDVI during this period were dominated by human activities. The reason is that after GGP initiation, the intensification of human activities, for example, projects such as returning farmland to forests and returning grazing land to grasslands, has become the dominant mechanism for NDVI changes in the YRB.

#### 3.4.2. Quantitative Analysis of the NDVI

This study first assumed (in Section 2.3.2) that human activities were weak in the $t_1$ (1982–1999) period, and then (in Section 3.4.1), we confirmed the relationship between the NDVI and climate change factors (precipitation and temperature) through qualitative analysis during this period close (correlation coefficients reached 0.84 and 0.88). Therefore, we further established the correlation equation between the NDVI and climate in the YRB during the $t_1$ period, and the relevant NDVI calculation formula can be found in Section 2.3.2. As shown in Table 5, in the YRB, the correlation coefficient between the NDVI and climate was as high as 0.88, which proves that our hypothesis is reasonable, and the contribution rate of human activities (59.3%) was greater than that of climate changes (40.7%). Except for two high-elevation sub-basins in the UYRB, the contribution rate of human activities in the other sub-basins exceeded 56%, and the correlation coefficients

were greater than 0.7, indicating that our results are reliable. Overall, the NDVI in most sub-basins was dominated by the human activities throughout the study period. From 1982 to 2019, the contribution rate of human activities to NDVI changes in the UYRB was only 35.6%, indicating that climate change was still the dominant factor. However, the contribution rate of human activities to vegetation coverage in the MYRB reached 79.5% during this period, possibly because MYRB is the main experimental area under the GGP, while the UYRB and the LYRB, which are on a high-altitude steep slope and a low-altitude shallow slope, respectively, are not.

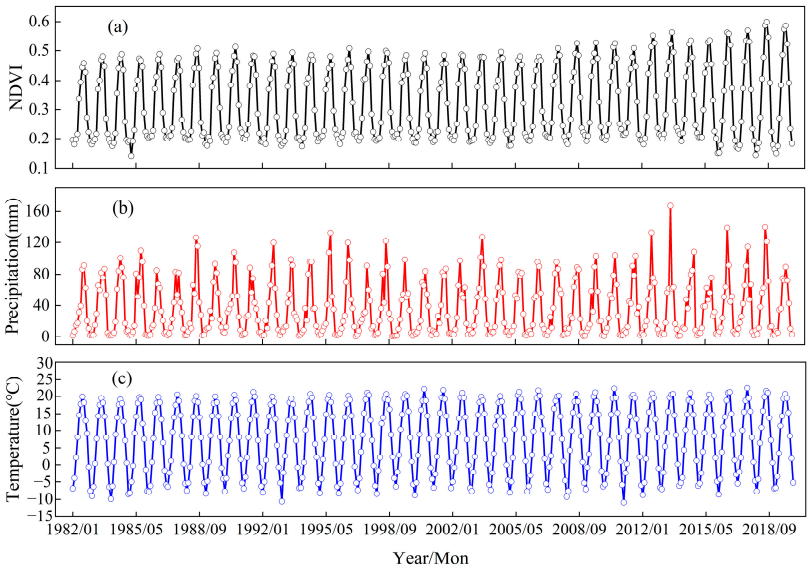


**Figure 10.** Temporal trend patterns of climate and the normal difference vegetation index (NDVI) in the Yellow River Basin (YRB). (**a**) NDVI, (**b**) precipitation (mm), and (**c**) temperature (°C).

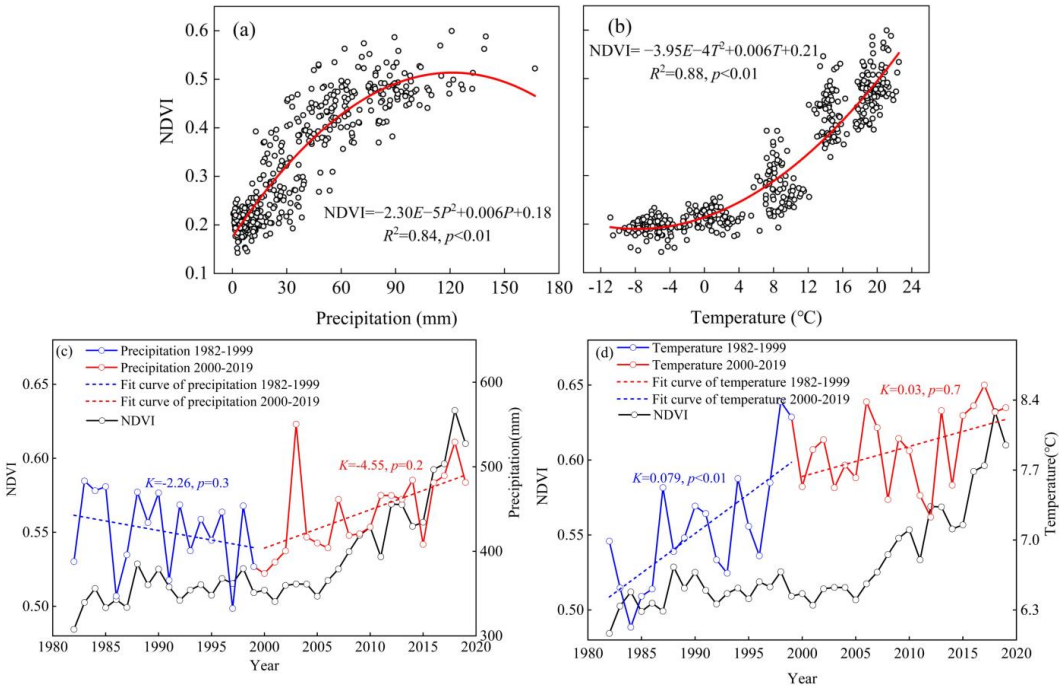


**Figure 11.** Qualitative analysis of the normal difference vegetation index (NDVI) and climate in the Yellow River Basin (YRB) from 1982 to 2019. (**a**) Analysis of the correlation between NDVI and precipitation, (**b**) analysis of the correlation between NDVI and temperature, (**c**) temporal variation in NDVI and precipitation, and (**d**) temporal variation in NDVI and temperature.

**Table 5.** Quantitative analysis of the YRB and sub-basins.

| Region | | NDVI versus Climate over $T_1$ Period | NDVI Change | | | Contribution (%) | |
|---|---|---|---|---|---|---|---|
| | | | $\overline{NDVI}_{t_1}$ | $\overline{NDVI}_{t_2}$ | $\Delta\overline{NDVI}_{tot}$ | $\Delta\overline{NDVI}_{CC}$ | $\Delta\overline{NDVI}_{HA}$ |
| YRB | | NDVI = 0.00128$P$ + 0.0070$T$ + 0.216 ($R^2$ = 0.88) | 0.5105 | 0.5795 | 0.0690 | 40.7 | 59.3 |
| UYRB | 1 | NDVI = 0.003$P$ + 0.0087$T$ + 0.27 ($R^2$ = 0.81) | 0.6633 | 0.6967 | 0.0334 | 55.2 | 44.8 |
| | 2 | NDVI = 0.00294$P$ + 0.0091$T$ + 0.235 ($R^2$ = 0.84) | 0.6563 | 0.6996 | 0.0433 | 71.1 | 28.9 |
| | 3 | NDVI = 0.00069$P$ + 0.0036$T$ + 0.128 ($R^2$ = 0.79) | 0.2757 | 0.3679 | 0.0922 | 23.3 | 76.7 |
| | 4 | NDVI = 0.00089$P$ + 0.003$T$ + 0.129 ($R^2$ = 0.82) | 0.2764 | 0.3509 | 0.0745 | 33 | 67 |
| MYRB | 5 | NDVI = 0.00063$P$ + 0.01$T$ + 0.244 ($R^2$ = 0.85) | 0.5984 | 0.6945 | 0.0961 | 34.6 | 65.4 |
| | 6 | NDVI = 0.00049$P$ + 0.0086$T$ + 0.232 ($R^2$ = 0.83) | 0.4976 | 0.6003 | 0.1027 | 25.1 | 74.9 |
| | 7 | NDVI = 0.00052$P$ + 0.003$T$ + 0.17 ($R^2$ = 0.73) | 0.3175 | 0.4447 | 0.1272 | 13 | 87 |
| | 8 | NDVI = 0.00061$P$ + 0.0013$T$ + 0.267 ($R^2$ = 0.85) | 0.6529 | 0.7208 | 0.0679 | 32.1 | 67.9 |
| | 9 | NDVI = 0.00046$P$ + 0.013$T$ + 0.302 ($R^2$ = 0.85) | 0.7033 | 0.7801 | 0.0768 | 21 | 79 |
| | 10 | NDVI = 0.00049$P$ + 0.013$T$ + 0.29 ($R^2$ = 0.90) | 0.6384 | 0.6948 | 0.0564 | 42.8 | 57.2 |
| | 11 | NDVI = 0.00052$P$ + 0.0037$T$ + 0.155 ($R^2$ = 0.70) | 0.3258 | 0.4658 | 0.1400 | 12 | 88 |
| | 12 | NDVI = 0.00021$P$ + 0.0166$T$ + 0.261 ($R^2$ = 0.89) | 0.7462 | 0.7750 | 0.0288 | 33.6 | 66.4 |
| LYRB | 13 | NDVI = 0.00049$P$ + 0.012$T$ + 0.257 ($R^2$ = 0.76) | 0.7285 | 0.7457 | 0.0172 | 28.7 | 71.3 |
| | 14 | NDVI = 0.00038$P$ + 0.013$T$ + 0.247 ($R^2$ = 0.84) | 0.6894 | 0.7132 | 0.0238 | 43.4 | 56.6 |

1–4 represent Datong, Huangshui, Shizuishan-Toudaoguai, and Xiaheyan-Shizuishan in the Upper Yellow River Basin (UYRB), respectively; 5–12 represent Fen, Jing, Kuye, Beiluo, Qin, Wei, Wuding, and Yiluo in the Middle Yellow River Basin (MYRB), respectively; and 13 and 14 represent Gaocun-Lijin and Upper daicunba in the Lower Yellow River Basin (LYRB), respectively. $t_1$ (1982–1999) and $t_2$ (2000–2019) represent the periods before and after the Grain for Green Program (GGP) initiation, respectively. $P$ and $T$ represent precipitation and temperature, respectively, and CC and HA represent climate change and human activities, respectively. NDVI: normal difference vegetation index.

## 4. Discussion

### *4.1. Variations in the Vegetation Coverage and the Factors Influencing It in the YRB*

Climate change and human activities are two important factors affecting regional vegetation coverage [31,32]. In this study, we selected 1999, the year in which the GGP was launched, and divided the long-term research scale into two sub-periods, $t_1$ (1982–1999) and $t_2$ (2000–2019), which are crucial for us to distinguish and discuss climate change and human activities. We assumed that before 1999, the change in the vegetation cover in the YRB was dominated by climate change, and then we reconstructed the relationship between the NDVI and climatic factors (precipitation and air temperature) under natural conditions. Calculation proved that before 1999, the vegetation cover in the YRB had a high correlation with climatic factors (precipitation and temperature) ($R^2$ = 0.84, $R^2$ = 0.88, and $p < 0.01$) (Figure 11a,b). We have developed equations that relate climatic elements to the NDVI under natural conditions ($R^2 \geq 0.70$) (Table 5). This is important for us to calculate the contribution rate of climate change and human activities to the vegetation cover in the YRB during the $t_2$ (2000–2019) sub-period.

The positive impact of the GGP on the vegetation cover in the YRB is considerable. Temporally, the fitting slope of the annual NDVI of the YRB from 2000 to 2019 (slope = 0.0067) is more than six times that of 1982–1999 (slope = 0.0011). So, the significance is $p < 0.05$ and $p < 0.01$. More than 80% of the sub-basins is consistent with the overall change trend of the YRB, and some even have a change rate of $t_2$ that is dozens of times that of $t_1$ (Figure 4b–d and Table 2). Spatially, the pattern change in the $t_2$ period was more obvious than that in the $t_1$ period, especially in the MYRB, because the MYRB is the key experimental area of the GGP (Figures 5 and 8). The land use in the YRB is mainly divided into three types: cultivated land, woodland, and grassland. The three areas and NDVI values remained basically unchanged before the initiation of the GGP but changed after 2000 (Figure 12). This indicates that the human activities represented by the GGP have a role in vegetation coverage in the YRB: a mechanism that positively affects vegetation coverage by converting land types.

Climate change can determine the large-area distribution pattern of vegetation through temperature regulation, precipitation input and output, and material and energy cycle conversion, while topographic elements, such as altitude and slope, can obviously affect the change of vegetation in small areas [33–35]. Human activities are increasingly occupying the main position among factors influencing vegetation cover change, represented by the GGP, whose contribution rate is as high as 59.3% since its inception (Table 5). In the YRB, the GGP is characterized by a wide range, sufficient power, and planning. Its aim is to transform the cultivated land with serious soil erosion, desertification, salinization, and rocky desertification into forest and grass and restore vegetation in the YRB [36,37]. Therefore, it has strong pertinence in vegetation cover restoration [38].

### *4.2. What Are the Contributions of the Vegetation Coverage Research?*

This study has developed a new research idea. In order to quantify the changes in vegetation cover in the YRB caused by climate change and human activities, the topographic elements of altitude and slope are introduced, which can better explain the spatial pattern of regional vegetation cover. This information will help us to make better decisions in the GGP regarding vegetation cover restoration.

First, for vegetation restoration, we need to adapt to local conditions and plan rationally. From the perspective of the overall distribution pattern of the NDVI in the YRB, the NDVI value is high in the southeast and low in the northwest (Figure 1f), caused by the spatial heterogeneity of natural climatic conditions in the YRB. Therefore, it is obviously unreasonable to blindly cultivate forest land in the northwest region and priority should be given to grassland. Numerous planted forests will lead to increased evaporation and decreased runoff, intensifying the drought in the arid regions of the YRB, which is already short of water [39]. This is also the reason why Figure 5 shows outliers in 2008 and recovery

later. Based on this, to have a positive impact, human activities need to adapt to different areas for vegetation cover restoration [40].

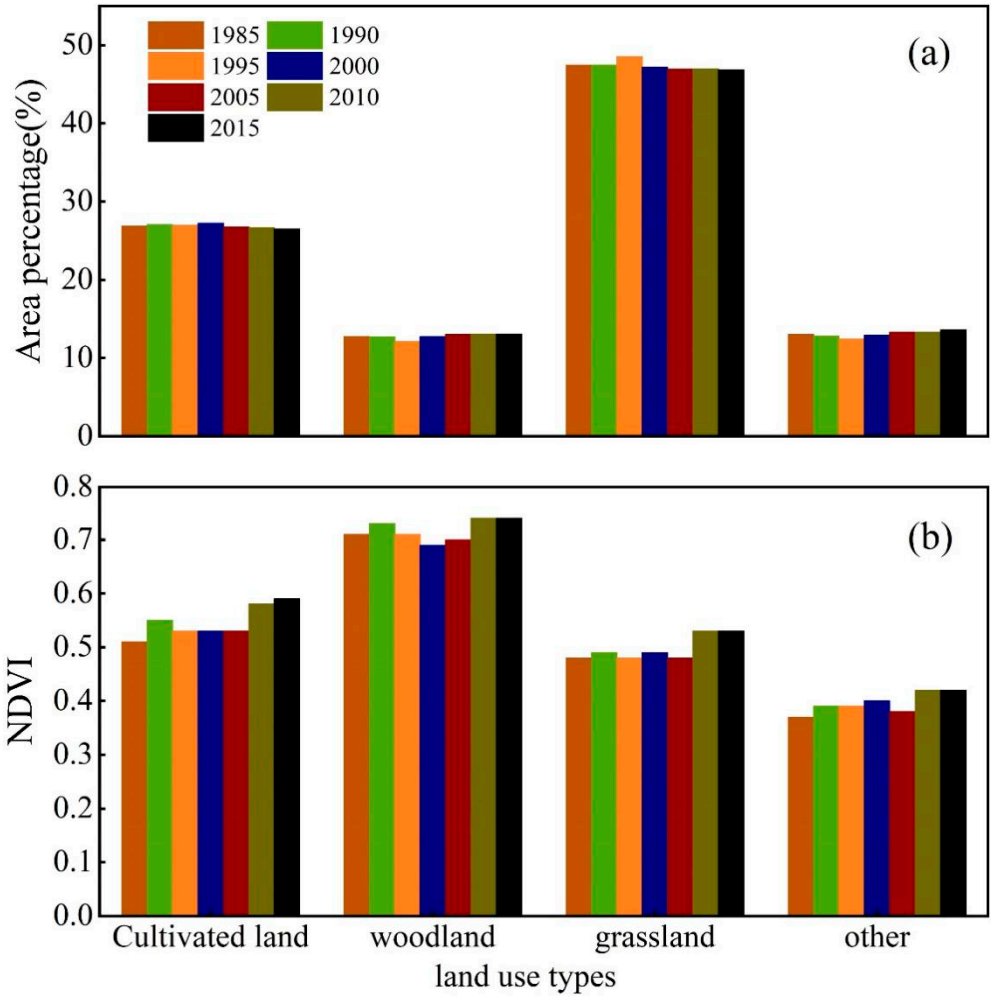


**Figure 12.** Temporal trend of land use types in the Yellow River Basin (YRB). (**a**) Proportion of land use area (%) and (**b**) the normal difference index (NDVI).

Furthermore, topographic factors have an important influence on vegetation types. In other words, vegetation has specific choices for the specific conditions of the topography, which can explain the rationality of specific vegetation-related NDVI changes in altitude and slope. For example, in Table 4, the high-level NDVIs of the sub-basins in the north of the MYRB are moving to a low slope, while the high-level NDVIs of the sub-basins in the south of the MYRB are moving to a high slope (Table 4), specifically because many hills and ravines in the northern part have farmlands while the southern part is mostly platform gully [36,38]. In addition to this, GGP's approach in the north is to convert steeply mountainous farmland into woodland in order to curb soil erosion [41]. Completely different, in the south, farmlands are being transformed into orchards and the like [42]. Hence, this is responsible for the variance in high-level NDVIs in diverse regions. The topographic factors introduced in this research can provide new ideas for interpreting the variation in the NDVI in different regions.

### *4.3. Limitations*

Although this study provides some usable ideas and methods, there are some limitations. At present, large-scale research based on remote sensing images and other spatial data is still limited by the low spatial–temporal resolution of the data and the small number

of meteorological stations. This situation will inevitably lead to errors in the accuracy of the study [18,20,23,43–46].

In addition, although the multivariate regression residual analysis method has been widely used to separate the effects of human activities on NDVI changes of vegetation, it still has some shortcomings [25]. For example, when establishing the multiple regression equation between climate elements and the NDVI, there is no conclusion on how to reasonably select climate elements (such as temperature, precipitation, and solar radiation). The number of selected factors may also be a limiting factor of the study, just as the few climate factors selected in this study may also cause certain errors [43].

Furthermore, specific aspects of human activities, such as agricultural technology progress and urban expansion, are not considered. To implement the GGP, we prefer to consider its overall effect on the YRB but do not reflect on more detailed issues [44]. Due to the difference in the responses of vegetation growth in different regions due to various influencing factors, the above problems and deficiencies are difficult to solve in large-scale research, resulting in certain uncertainty in the research results [45,46].

## 5. Conclusions

This study introduces and analyzes the difference in spatial–temporal changes in two different sub-periods, $t_1$ (1982–1999) and $t_2$ (2000–2019), in the YRB. In the $t_2$ period, with significant human activities ($p < 0.01$), the NDVI change rate is more than six times that in $t_1$ and the contribution rate of human activities in most sub-basin areas is greater than 50%. The dominant factor influencing vegetation cover change from $t_1$ to $t_2$ gradually transited from climate change to human activities. After the initiation of the GGP, low-level NDVIs gradually advanced to higher altitudes, high-level NDVIs moved to lower altitudes, and more low-level NDVIs were transformed to high values. The areas of high-level NDVIs in the southeast of the YRB are gradually expanding to the northwest.

This research also innovatively introduced topographic elements to analyze the distribution pattern of vegetation change, which provided some knowledge related to vegetation coverage in the region. However, in future works, refining the driving factors of vegetation change, determining the relationship between each factor and vegetation change, and evaluating the accuracy of the results through field surveys will help reduce the above uncertainties. In terms of method, more theories conducive to detailed analysis of the driving factors of vegetation cover need to be developed. In general, further research is desired related to the impact of human activities and climate changes on vegetation cover change in the YRB and its driving mechanism.

**Author Contributions:** Conceptualization, Q.Z. and S.J.; methodology, Q.Z.; software, Q.Z.; validation, Q.Z. and H.W.; formal analysis, Q.Z. and S.J.; investigation, H.W.; resources, Q.Z.; data curation, S.J.; writing—original draft preparation, Q.Z. and S.J.; writing—review and editing, H.W.; visualization, H.W.; supervision, H.W.; project administration, Q.Z.; funding acquisition, S.J. All authors have read and agreed to the published version of the manuscript.

**Funding:** This research was funded by the Training Program for Young Backbone Teachers in Colleges and Universities of Henan Province (2021GGJS003), the Henan Natural Science Foundation (212300410413), the Henan Youth Talent Promotion Project (2021HYTP030), China Postdoctoral Science Foundation (2020M672247), and major scientific and technological projects of Henan Province, China (201300311400).

**Institutional Review Board Statement:** No applicable.

**Informed Consent Statement:** No applicable.

**Data Availability Statement:** Not applicable.

**Conflicts of Interest:** The authors declare no conflict of interest.

## References


1. Klimavičius, L.; Rimkus, E.; Stonevičius, E.; Mačiulytė, V. Seasonality and long-term trends of NDVI values in different land use types in the eastern part of the Baltic Sea basin. *Oceanologia* **2022**. [CrossRef]
2. Han, J.C.; Huang, Y.F.; Zhang, H.; Wu, X.F. Characterization of elevation and land cover dependent trends of NDVI variations in the Hexi region, northwest China. *J. Environ. Manag.* **2019**, *232*, 1037–1048. [CrossRef] [PubMed]
3. Feng, X.M.; Fu, B.J.; Piao, S.L.; Wang, S.H.; Ciais, P.; Zeng, Z.Z.; Lu, Y.H.; Zeng, Y.; Li, Y.; Jiang, X.H.; et al. Revegetation in China's Loess Plateau is approaching sustainable water resource limits. *Nat. Clim. Chang.* **2016**, *6*, 1019–1022. [CrossRef]
4. Li, J.J.; Peng, S.Z.; Li, Z. Detecting and attributing vegetation changes on China's Loess Plateau. *Agric. For. Meteorol.* **2017**, *247*, 260–270. [CrossRef]
5. Feng, T.; Liu, L.Z.; Yang, J.H.; Wu, J.J. Vegetation greening in more than 94% of the Yellow River Basin (YRB) region in China during the 21st century caused jointly by warming and anthropogenic activities. *Ecol. Indic.* **2021**, *125*, 107479. [CrossRef]
6. Zhao, G.J.; Tian, P.; Mu, X.M.; Jiao, J.Y.; Wang, F.; Gao, P. Quantifying the impact of climate variability and human activities on streamflow in the middle reaches of the Yellow River basin, China. *J. Hydrol.* **2014**, *519*, 387–398. [CrossRef]
7. Sun, W.Y.; Song, X.Y.; Mu, X.M.; Gao, P.; Wang, F.; Zhao, G.J. Spatiotemporal vegetation cover variations associated with climate change and ecological restoration in the Loess Plateau. *Agric. For. Meteorol.* **2015**, *209–210*, 87–99. [CrossRef]
8. Peng, L.; Wang, J.; Liu, M.M.; Xue, Z.H.; Bagherzadeh, A.; Liu, M.Y. Spatio-temporal variation characteristics of NDVI and its response to climate on the Loess Plateau from 1985 to 2015. *Catena* **2021**, *203*, 105331. [CrossRef]
9. Ma, Q.M.; Long, Y.P.; Jia, X.P.; Wang, H.B.; Li, Y.S. Vegetation response to climatic variation and human activities on the Ordos Plateau from 2000 to 2016. *Environ. Earth Sci.* **2019**, *78*, 709. [CrossRef]
10. Wang, Y.Q.; Shao, M.A.; Zhu, Y.J.; Liu, Z.P. Impacts of land use and plant characteristics on dried soil layers in different climatic regions on the Loess Plateau of China. *Agric. For. Meteorol.* **2011**, *151*, 437–448. [CrossRef]
11. Wang, J.J.; Liu, Z.P.; Gao, J.L.; Emanuele, L.; Ren, Y.Q.; Shao, M.A.; Wei, X.R. The Grain for Green project eliminated the effect of soil erosion on organic carbon on China's Loess Plateau between 1980 and 2008. *Agric. Ecosyst. Environ.* **2021**, *322*, 107636. [CrossRef]
12. Fensholt, R.; Proud, S.R. Evaluation of Earth Observation based global long term vegetation trends—Comparing GIMMS and MODIS global NDVI time series. *Remote Sens. Environ.* **2012**, *119*, 131–147. [CrossRef]
13. Cramer, W.; Bondeau, A.; Woodward, F.I.; Prentice, I.C.; Betts, R.A.; Brovkin, V.; Cox, P.M.; Fisher, V.; Foley, J.A.; Friend, A.D.; et al. Global response of terrestrial ecosystem structure and function to $CO_2$ and climate change: Results from six dynamic global vegetation models. *Glob. Chang. Biol.* **2001**, *7*, 357–373. [CrossRef]
14. Theurillat, J.P.; Guisan, A. Potential Impact of Climate Change on Vegetation in the European Alps: A Review. *Clim. Chang.* **2001**, *50*, 77–109. [CrossRef]
15. Chen, Z.; Liu, J.Y.; Li, L.; Wu, Y.P.; Feng, G.L.; Qian, Z.H.; Sun, G.Q. Effects of climate change on vegetation patterns in Hulun Buir Grassland. *Phys. A Stat. Mech. Appl.* **2022**, *597*, 127275. [CrossRef]
16. Brown, D.G. Comparison of vegetation-topography relationships at the Alpine treeline ecotone. *Phys. Geogr.* **1994**, *15*, 125–145. [CrossRef]
17. Fu, B.J.; Zhang, Q.J.; Chen, L.D.; Zhao, W.W.; Gulinck, H.; Liu, G.B.; Yang, Q.K.; Zhu, Y.G. Temporal change in land use and its relationship to slope degree and soil type in a small catchment on the Loess Plateau of China. *Catena* **2006**, *65*, 41–48. [CrossRef]
18. Liu, Z.J.; Wang, J.Y.; Wang, X.Y.; Wang, Y.S. Understanding the impacts of 'Grain for Green' land management practice on land greening dynamics over the Loess Plateau of China. *Land Use Policy* **2020**, *99*, 105084. [CrossRef]
19. Zhao, A.Z.; Zhang, A.B.; Liu, J.H.; Feng, L.L.; Zhao, Y.L. Assessing the effects of drought and "Grain for Green" Program on vegetation dynamics in China's Loess Plateau from 2000 to 2014. *Catena* **2019**, *175*, 446–455. [CrossRef]
20. Ren, Z.; Tian, Z.; Wei, H.; Liu, Y.; Yu, Y. Spatiotemporal evolution and driving mechanisms of vegetation in the Yellow River Basin, China during 2000–2020. *Ecol. Indic.* **2022**, *138*, 108832. [CrossRef]
21. Liu, C.; Zhang, X.; Wang, T.; Chen, G.; Zhu, K.; Wang, Q.; Wang, J. Detection of vegetation coverage changes in the Yellow River Basin from 2003 to 2020. *Ecol. Indic.* **2022**, *138*, 108818. [CrossRef]
22. Zhu, L.J.; Meng, J.J.; Zhu, L.K. Applying Geodetector to disentangle the contributions of natural and anthropogenic factors to NDVI variations in the middle reaches of the Heihe River Basin. *Ecol. Indic.* **2020**, *117*, 106545. [CrossRef]
23. Zewdie, W.; Csaplovics, E.; Inostroza, L. Monitoring ecosystem dynamics in northwestern Ethiopia using NDVI and climate variables to assess long term trends in dryland vegetation variability. *Appl. Geogr.* **2017**, *79*, 167–178. [CrossRef]
24. Fensholt, R.; Rasmussen, K.; Nielsen, T.T.; Mbow, C. Evaluation of earth observation based long term vegetation trends—Intercomparing NDVI time series trend analysis consistency of Sahel from AVHRR GIMMS, Terra MODIS and SPOT VGT data. *Remote Sens. Environ.* **2009**, *113*, 1886–1898. [CrossRef]
25. Kong, D.X.; Miao, C.Y.; Wu, J.W.; Duan, Q.Y. Impact assessment of climate change and human activities on net runoff in the Yellow River Basin from 1951 to 2012. *Ecol. Eng.* **2016**, *91*, 566–573. [CrossRef]
26. Hu, Y.G.; Li, H.; Wu, D.; Chen, W.; Zhao, X.; Hou, M.L.; Li, A.J.; Zhu, Y.J. LAI-indicated vegetation dynamic in ecologically fragile region: A case study in the Three-North Shelter Forest program region of China. *Ecol. Indic.* **2021**, *120*, 106932. [CrossRef]
27. Nikolakopoulos, K.G.; Kamaratakis, E.K.; Chrysoulakis, N. SRTM vs ASTER elevation products. Comparison for two regions in Crete, Greece. *Int. J. Remote Sens.* **2006**, *27*, 4819–4838. [CrossRef]

28. Jing, C.W.; Shortridge, A.; Lin, S.P.; Wu, J.P. Comparison and validation of SRTM and ASTER GDEM for a subtropical landscape in Southeastern China. *Int. J. Digit. Earth.* **2014**, *7*, 969–992. [CrossRef]
29. Carlson, T.N.; Ripley, D.A. On the relation between NDVI, fractional vegetation cover, and leaf area index. *Remote Sens. Environ.* **1997**, *62*, 241–252. [CrossRef]
30. Guo, B.; Wei, C.X.; Yu, Y.; Liu, Y.F.; Li, J.L.; Meng, C.; Cai, Y.M. The dominant influencing factors of desertification changes in the source region of Yellow River: Climate change or human activity? *Sci. Total Environ.* **2022**, *813*, 152512. [CrossRef]
31. Qian, C.; Shao, L.Q.; Hou, X.H.; Zhang, B.B.; Chen, W.; Xia, X.L. Detection and attribution of vegetation greening trend across distinct local landscapes under China's Grain to Green Program: A case study in Shaanxi Province. *Catena* **2019**, *183*, 104182. [CrossRef]
32. Sun, J.Q.; Wang, X.J.; Shahid, S.; Yin, Y.X.; Li, E. Spatiotemporal changes in water consumption structure of the Yellow River Basin, China. *Phys. Chem. Earth Parts A/B/C* **2022**, *126*, 103112. [CrossRef]
33. Omer, A.; Elagib, N.A.; Ma, Z.G.; Saleem, F.; Mohammed, A. Water scarcity in the Yellow River Basin under future climate change and human activities. *Sci. Total Environ.* **2020**, *749*, 141446. [CrossRef] [PubMed]
34. Xie, J.K.; Xu, Y.P.; Wang, Y.T.; Gu, H.T.; Wang, F.M.; Pan, S.L. Influences of climatic variability and human activities on terrestrial water storage variations across the Yellow River basin in the recent decade. *J. Hydrol.* **2019**, *579*, 124218. [CrossRef]
35. Bao, Z.X.; Zhang, J.Y.; Wang, G.Q.; Chen, Q.W.; Guan, T.S.; Yan, X.L.; Liu, C.S.; Liu, J.; Wang, J. The impact of climate variability and land use/cover change on the water balance in the Middle Yellow River Basin, China. *J. Hydrol.* **2019**, *577*, 123942. [CrossRef]
36. Li, C.C.; Zhang, Y.Q.; Shen, Y.J.; Yu, Q. Decadal water storage decrease driven by vegetation changes in the Yellow River Basin. *Sci. Bull.* **2020**, *65*, 1859–1861. [CrossRef]
37. Wu, Q.S.; Zuo, Q.T.; Han, C.H.; Ma, J.X. Integrated assessment of variation characteristics and driving forces in precipitation and temperature under climate change: A case study of Upper Yellow River basin, China. *Atmos. Res.* **2020**, *272*, 106156. [CrossRef]
38. Yang, Z.F.; Yan, Y.; Liu, Q. The relationship of Streamflow-Precipitation-Temperature in the Yellow River Basin of China during 1961-2000. *Procedia Environ. Sci.* **2012**, *13*, 2336–2345. [CrossRef]
39. Wang, Y.P.; Wang, S.; Wang, C.; Zhao, W.W. Runoff sensitivity increases with land use/cover change contributing to runoff decline across the middle reaches of the Yellow River basin. *J. Hydrol.* **2021**, *600*, 126536. [CrossRef]
40. Wang, D.L.; Feng, H.M.; Zhang, B.Z.; Wei, Z.; Tian, Y.L. Quantifying the impacts of climate change and vegetation change on decreased runoff in China's yellow river basin. *Ecohydrol. Hydrobiol.* **2022**, *22*, 310–322. [CrossRef]
41. Sun, Z.D.; Chang, N.B.; Opp, C.; Hennig, T. Evaluation of ecological restoration through vegetation patterns in the lower Tarim River, China with MODIS NDVI data. *Ecol. Inform.* **2011**, *6*, 156–163. [CrossRef]
42. Zhao, J.; Huang, S.Z.; Huang, Q.; Wang, H.; Leng, G.Y.; Fang, W. Time-lagged response of vegetation dynamics to climatic and teleconnection factors. *Catena* **2020**, *189*, 104474. [CrossRef]
43. Xu, S.Q.; Yu, Z.B.; Yang, C.G.; Ji, X.B.; Zhang, K. Trends in evapotranspiration and their responses to climate change and vegetation greening over the upper reaches of the Yellow River Basin. *Agric. For. Meteorol.* **2018**, *263*, 118–129. [CrossRef]
44. Mathieu, D.; Roberto, O.C.; Katarina, Č.; Sergio, A.E.; Jan, G.P.W.C.; Peter, P.; Jožica, G.; Zalika, Č.; Maks, M.; Martin, D.L.; et al. Spatio-temporal assessment of beech growth in relation to climate extremes in Slovenia—An integrated approach using remote sensing and tree-ring data. *Agric. For. Meteorol.* **2020**, *287*, 107925. [CrossRef]
45. Shen, X.J.; Liu, B.H.; Henderson, M.; Wang, L.; Jiang, M.; Lu, X.G. Vegetation Greening, Extended Growing Seasons, and Temperature Feedbacks in Warming Temperate Grasslands of China. *J. Clim.* **2022**, *35*, 5103–5117. [CrossRef]
46. Jin, N.; Tao, B.; Ren, W.; He, L.; Zhang, D.; Wang, D.; Yu, Q. Assimilating remote sensing data into a crop model improves winter wheat yield estimation based on regional irrigation data. *Agric. Water Manag.* **2022**, *266*, 107583. [CrossRef]